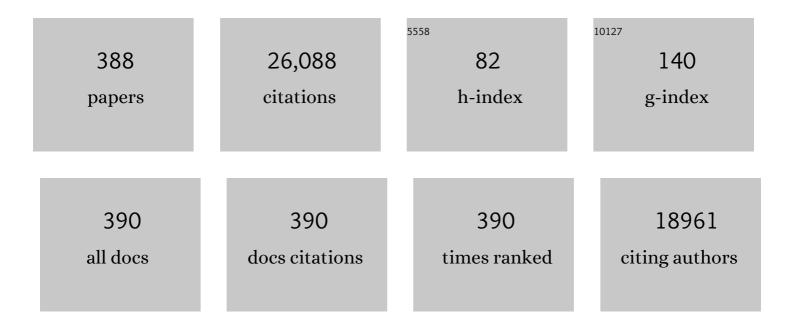
Cheng Yan

List of Publications by Year in descending order

Source: https://exaly.com/author-pdf/6164252/publications.pdf Version: 2024-02-01



CHENC YAN

#	Article	IF	CITATIONS
1	A Hierarchical Z‑Scheme αâ€Fe ₂ O ₃ /gâ€C ₃ N ₄ Hybrid for Enhanced Photocatalytic CO ₂ Reduction. Advanced Materials, 2018, 30, 1706108.	11.1	761
2	High Efficiency Photocatalytic Water Splitting Using 2D αâ€Fe ₂ 0 ₃ /gâ€C ₃ N ₄ Zâ€6cheme Catalysts. Advanced Energ Materials, 2017, 7, 1700025.	y 10.2	664
3	Novel visible-light-driven CQDs/Bi 2 WO 6 hybrid materials with enhanced photocatalytic activity toward organic pollutants degradation and mechanism insight. Applied Catalysis B: Environmental, 2015, 168-169, 51-61.	10.8	486
4	Surface Defect Engineering in 2D Nanomaterials for Photocatalysis. Advanced Functional Materials, 2018, 28, 1801983.	7.8	472
5	Preparation of sphere-like g-C3N4/BiOI photocatalysts via a reactable ionic liquid for visible-light-driven photocatalytic degradation of pollutants. Journal of Materials Chemistry A, 2014, 2, 5340.	5.2	439
6	Bismuth oxyhalide layered materials for energy and environmental applications. Nano Energy, 2017, 41, 172-192.	8.2	413
7	Ultrathin 2D Photocatalysts: Electronicâ€Structure Tailoring, Hybridization, and Applications. Advanced Materials, 2018, 30, 1704548.	11.1	409
8	lonic liquid-induced strategy for carbon quantum dots/BiOX (X = Br, Cl) hybrid nanosheets with superior visible light-driven photocatalysis. Applied Catalysis B: Environmental, 2016, 181, 260-269.	10.8	380
9	Oxygenated monolayer carbon nitride for excellent photocatalytic hydrogen evolution and external quantum efficiency. Nano Energy, 2016, 27, 138-146.	8.2	379
10	Electrochemical CO ₂ Reduction with Atomic Ironâ€Đispersed on Nitrogenâ€Doped Graphene. Advanced Energy Materials, 2018, 8, 1703487.	10.2	369
11	Exfoliated graphene-like carbon nitride in organic solvents: enhanced photocatalytic activity and highly selective and sensitive sensor for the detection of trace amounts of Cu2+. Journal of Materials Chemistry A, 2014, 2, 2563.	5.2	330
12	Defectâ€Rich Bi ₁₂ O ₁₇ Cl ₂ Nanotubes Selfâ€Accelerating Charge Separation for Boosting Photocatalytic CO ₂ Reduction. Angewandte Chemie - International Edition, 2018, 57, 14847-14851.	7.2	329
13	Isolated single atom cobalt in Bi3O4Br atomic layers to trigger efficient CO2 photoreduction. Nature Communications, 2019, 10, 2840.	5.8	327
14	Defectâ€Tailoring Mediated Electron–Hole Separation in Singleâ€Unitâ€Cell Bi ₃ O ₄ Br Nanosheets for Boosting Photocatalytic Hydrogen Evolution and Nitrogen Fixation. Advanced Materials, 2019, 31, e1807576.	11.1	311
15	Controlled Gas Exfoliation of Boron Nitride into Fewâ€Layered Nanosheets. Angewandte Chemie - International Edition, 2016, 55, 10766-10770.	7.2	271
16	Porous nitrogen-rich g-C3N4 nanotubes for efficient photocatalytic CO2 reduction. Applied Catalysis B: Environmental, 2019, 256, 117854.	10.8	271
17	MoS ₂ /TiO ₂ Edgeâ€On Heterostructure for Efficient Photocatalytic Hydrogen Evolution. Advanced Energy Materials, 2016, 6, 1600464.	10.2	264
18	Synthesis of magnetic CoFe2O4/g-C3N4 composite and its enhancement of photocatalytic ability under visible-light. Colloids and Surfaces A: Physicochemical and Engineering Aspects, 2015, 478, 71-80.	2.3	253

#	Article	IF	CITATIONS
19	Atomically-thin Bi2MoO6 nanosheets with vacancy pairs for improved photocatalytic CO2 reduction. Nano Energy, 2019, 61, 54-59.	8.2	243
20	One-pot extraction combined with metal-free photochemical aerobic oxidative desulfurization in deep eutectic solvent. Green Chemistry, 2015, 17, 2464-2472.	4.6	232
21	Ultrathin two-dimensional materials for photo- and electrocatalytic hydrogen evolution. Materials Today, 2018, 21, 749-770.	8.3	228
22	Commercially available molybdic compound-catalyzed ultra-deep desulfurization of fuels in ionic liquids. Green Chemistry, 2008, 10, 641.	4.6	214
23	Construction of core-shell heterojunction regulating α-Fe2O3 layer on CeO2 nanotube arrays enables highly efficient Z-scheme photoelectrocatalysis. Applied Catalysis B: Environmental, 2020, 276, 119138.	10.8	210
24	A template-free solvent-mediated synthesis of high surface area boron nitride nanosheets for aerobic oxidative desulfurization. Chemical Communications, 2016, 52, 144-147.	2.2	206
25	Controllable synthesis of Bi ₄ O ₅ Br ₂ ultrathin nanosheets for photocatalytic removal of ciprofloxacin and mechanism insight. Journal of Materials Chemistry A, 2015, 3, 15108-15118.	5.2	202
26	Taming interfacial electronic properties of platinum nanoparticles on vacancy-abundant boron nitride nanosheets for enhanced catalysis. Nature Communications, 2017, 8, 15291.	5.8	200
27	Nature-based catalyst for visible-light-driven photocatalytic CO ₂ reduction. Energy and Environmental Science, 2018, 11, 2382-2389.	15.6	198
28	Reactable ionic liquid-assisted rapid synthesis of BiOI hollow microspheres at room temperature with enhanced photocatalytic activity. Journal of Materials Chemistry A, 2014, 2, 15864-15874.	5.2	196
29	Recent Progress of Carbon-Supported Single-Atom Catalysts for Energy Conversion and Storage. Matter, 2020, 3, 1442-1476.	5.0	196
30	Oxidative Desulfurization of Fuels Catalyzed by Peroxotungsten and Peroxomolybdenum Complexes in lonic Liquids. Energy & Fuels, 2007, 21, 2514-2516.	2.5	195
31	The selectivity for sulfur removal from oils: An insight from conceptual density functional theory. AICHE Journal, 2016, 62, 2087-2100.	1.8	192
32	Freestanding atomically-thin two-dimensional materials beyond graphene meeting photocatalysis: Opportunities and challenges. Nano Energy, 2017, 35, 79-91.	8.2	179
33	Synthesis of g-C ₃ N ₄ at different temperatures for superior visible/UV photocatalytic performance and photoelectrochemical sensing of MB solution. RSC Advances, 2015, 5, 101552-101562.	1.7	175
34	Facile fabrication of the visible-light-driven Bi ₂ WO ₆ /BiOBr composite with enhanced photocatalytic activity. RSC Advances, 2014, 4, 82-90.	1.7	174
35	Bismuth vacancy mediated single unit cell Bi2WO6 nanosheets for boosting photocatalytic oxygen evolution. Applied Catalysis B: Environmental, 2018, 238, 119-125.	10.8	173
36	Synthesis and characterization of CeO2/g-C3N4 composites with enhanced visible-light photocatatalytic activity. RSC Advances, 2013, 3, 22269.	1.7	170

#	Article	IF	CITATIONS
37	Few-layered graphene-like boron nitride induced a remarkable adsorption capacity for dibenzothiophene in fuels. Green Chemistry, 2015, 17, 1647-1656.	4.6	167
38	A g-C3N4/BiOBr visible-light-driven composite: synthesis via a reactable ionic liquid and improved photocatalytic activity. RSC Advances, 2013, 3, 19624.	1.7	162
39	Constructing confined surface carbon defects in ultrathin graphitic carbon nitride for photocatalytic free radical manipulation. Carbon, 2016, 107, 1-10.	5.4	159
40	Emerging surface strategies on graphitic carbon nitride for solar driven water splitting. Chemical Engineering Journal, 2020, 382, 122812.	6.6	155
41	Deep oxidative desulfurization of fuels in redox ionic liquids based on iron chloride. Green Chemistry, 2009, 11, 810.	4.6	152
42	Boric acid-based ternary deep eutectic solvent for extraction and oxidative desulfurization of diesel fuel. Green Chemistry, 2019, 21, 3074-3080.	4.6	151
43	Construction of a 2D Grapheneâ€Like MoS ₂ /C ₃ N ₄ Heterojunction with Enhanced Visibleâ€Light Photocatalytic Activity and Photoelectrochemical Activity. Chemistry - A European Journal, 2016, 22, 4764-4773.	1.7	149
44	Bismuth Vacancy-Tuned Bismuth Oxybromide Ultrathin Nanosheets toward Photocatalytic CO ₂ Reduction. ACS Applied Materials & Interfaces, 2019, 11, 30786-30792.	4.0	140
45	Carbon Quantum Dots Induced Ultrasmall BiOI Nanosheets with Assembled Hollow Structures for Broad Spectrum Photocatalytic Activity and Mechanism Insight. Langmuir, 2016, 32, 2075-2084.	1.6	136
46	Taming electronic properties of boron nitride nanosheets as metal-free catalysts for aerobic oxidative desulfurization of fuels. Green Chemistry, 2018, 20, 4453-4460.	4.6	128
47	Carbon-doped porous boron nitride: metal-free adsorbents for sulfur removal from fuels. Journal of Materials Chemistry A, 2015, 3, 12738-12747.	5.2	126
48	Bidirectional acceleration of carrier separation spatially via N-CQDs/atomically-thin BiOI nanosheets nanojunctions for manipulating active species in a photocatalytic process. Journal of Materials Chemistry A, 2016, 4, 5051-5061.	5.2	126
49	Different Morphologies of SnS ₂ Supported on 2D g-C ₃ N ₄ for Excellent and Stable Visible Light Photocatalytic Hydrogen Generation. ACS Sustainable Chemistry and Engineering, 2018, 6, 5132-5141.	3.2	125
50	Spaceâ€Confined Yolkâ€Shell Construction of Fe ₃ O ₄ Nanoparticles Inside Nâ€Doped Hollow Mesoporous Carbon Spheres as Bifunctional Electrocatalysts for Longâ€Term Rechargeable Zinc–Air Batteries. Advanced Functional Materials, 2020, 30, 2005834.	7.8	119
51	Phosphotungstic Acid Immobilized on Ionic Liquid-Modified SBA-15: Efficient Hydrophobic Heterogeneous Catalyst for Oxidative Desulfurization in Fuel. Industrial & Engineering Chemistry Research, 2014, 53, 19895-19904.	1.8	118
52	Cobalt nitride as a novel cocatalyst to boost photocatalytic CO2 reduction. Nano Energy, 2021, 79, 105429.	8.2	117
53	Deep oxidative desulfurization of fuels by Fenton-like reagent in ionic liquids. Green Chemistry, 2009, 11, 1801.	4.6	115
54	Catalytic oxidative desulfurization with a hexatungstate/aqueous H2O2/ionic liquid emulsion system. Green Chemistry, 2011, 13, 1210.	4.6	115

#	Article	IF	CITATIONS
55	A sensitive signal-on photoelectrochemical sensor for tetracycline determination using visible-light-driven flower-like CN/BiOBr composites. Biosensors and Bioelectronics, 2018, 111, 74-81.	5.3	115
56	In-situ preparation of NH2-MIL-125(Ti)/BiOCl composite with accelerating charge carriers for boosting visible light photocatalytic activity. Applied Surface Science, 2019, 466, 525-534.	3.1	113
57	N-CQDs accelerating surface charge transfer of Bi4O5I2 hollow nanotubes with broad spectrum photocatalytic activity. Applied Catalysis B: Environmental, 2018, 237, 1033-1043.	10.8	112
58	Ultrathin g-C3N4 with enriched surface carbon vacancies enables highly efficient photocatalytic nitrogen fixation. Journal of Colloid and Interface Science, 2019, 553, 530-539.	5.0	112
59	One-pot solvothermal synthesis of Cu-modified BiOCl via a Cu-containing ionic liquid and its visible-light photocatalytic properties. RSC Advances, 2014, 4, 14281.	1.7	111
60	Magnetic g-C ₃ N ₄ /NiFe ₂ O ₄ hybrids with enhanced photocatalytic activity. RSC Advances, 2015, 5, 57960-57967.	1.7	110
61	Metal-Oxide-Mediated Subtractive Manufacturing of Two-Dimensional Carbon Nitride for High-Efficiency and High-Yield Photocatalytic H ₂ Evolution. ACS Nano, 2019, 13, 11294-11302.	7.3	109
62	Surface Local Polarization Induced by Bismuthâ€Oxygen Vacancy Pairs Tuning Nonâ€Covalent Interaction for CO ₂ Photoreduction. Advanced Energy Materials, 2021, 11, 2102389.	10.2	109
63	Controllable Synthesis of Atomically Thin Typeâ€II Weyl Semimetal WTe ₂ Nanosheets: An Advanced Electrode Material for Allâ€Solidâ€State Flexible Supercapacitors. Advanced Materials, 2017, 29, 1701909.	11.1	107
64	Defect engineering in atomically-thin bismuth oxychloride towards photocatalytic oxygen evolution. Journal of Materials Chemistry A, 2017, 5, 14144-14151.	5.2	107
65	Magnetic mesoporous nanospheres supported phosphomolybdate-based ionic liquid for aerobic oxidative desulfurization of fuel. Journal of Colloid and Interface Science, 2019, 534, 239-247.	5.0	106
66	Vibrational analysis and formation mechanism of typical deep eutectic solvents: An experimental and theoretical study. Journal of Molecular Graphics and Modelling, 2016, 68, 158-175.	1.3	105
67	Deep Oxidative Desulfurization of Fuel Oils Catalyzed by Decatungstates in the Ionic Liquid of [Bmim]PF6. Industrial & Engineering Chemistry Research, 2009, 48, 9034-9039.	1.8	102
68	Biomass willow catkin-derived Co ₃ O ₄ /N-doped hollow hierarchical porous carbon microtubes as an effective tri-functional electrocatalyst. Journal of Materials Chemistry A, 2017, 5, 20170-20179.	5.2	102
69	Hierarchical Sandwich-Like Structure of Ultrafine N-Rich Porous Carbon Nanospheres Grown on Graphene Sheets as Superior Lithium-Ion Battery Anodes. ACS Applied Materials & Interfaces, 2016, 8, 10324-10333.	4.0	100
70	Multiple Active Sites of Carbon for Highâ€Rate Surfaceâ€Capacitive Sodiumâ€lon Storage. Angewandte Chemie - International Edition, 2019, 58, 13584-13589.	7.2	98
71	Boron Nitride Mesoporous Nanowires with Doped Oxygen Atoms for the Remarkable Adsorption Desulfurization Performance from Fuels. ACS Sustainable Chemistry and Engineering, 2016, 4, 4457-4464.	3.2	95
72	Ultrathin structured photocatalysts: A versatile platform for CO2 reduction. Applied Catalysis B: Environmental, 2019, 256, 117788.	10.8	94

#	Article	IF	CITATIONS
73	Sacrificing ionic liquid-assisted anchoring of carbonized polymer dots on perovskite-like PbBiO2Br for robust CO2 photoreduction. Applied Catalysis B: Environmental, 2019, 254, 551-559.	10.8	91
74	Reversible Formation of gâ€C ₃ N ₄ 3D Hydrogels through Ionic Liquid Activation: Gelation Behavior and Roomâ€Temperature Gasâ€Sensing Properties. Advanced Functional Materials, 2017, 27, 1700653.	7.8	90
75	Freestanding ultrathin bismuth-based materials for diversified photocatalytic applications. Journal of Materials Chemistry A, 2019, 7, 25203-25226.	5.2	90
76	A plasmonic photocatalyst of Ag/AgBr nanoparticles coupled with g-C3N4 with enhanced visible-light photocatalytic ability. Colloids and Surfaces A: Physicochemical and Engineering Aspects, 2013, 436, 474-483.	2.3	89
77	Rapid synthesis of ultrathin 2D materials through liquid-nitrogen and microwave treatments. Journal of Materials Chemistry A, 2019, 7, 5209-5213.	5.2	89
78	Enhanced Photocatalytic Activity of Ag ₃ VO ₄ Loaded with Rare-Earth Elements under Visible-Light Irradiation. Industrial & Engineering Chemistry Research, 2009, 48, 10771-10778.	1.8	88
79	A DFT Study of the Extractive Desulfurization Mechanism by [BMIM] ⁺ [AlCl ₄] ^{â^'} Ionic Liquid. Journal of Physical Chemistry B, 2015, 119, 5995-6009.	1.2	88
80	Tuning the Chemical Hardness of Boron Nitride Nanosheets by Doping Carbon for Enhanced Adsorption Capacity. ACS Omega, 2017, 2, 5385-5394.	1.6	86
81	Controllable synthesis of uniform mesoporous H-Nb ₂ O ₅ /rGO nanocomposites for advanced lithium ion hybrid supercapacitors. Journal of Materials Chemistry A, 2019, 7, 693-703.	5.2	86
82	Improved visible light photocatalytic properties of Fe/BiOCl microspheres synthesized via self-doped reactable ionic liquids. CrystEngComm, 2013, 15, 10132.	1.3	84
83	Visible-light-driven Ag/AgBr/ZnFe2O4 composites with excellent photocatalytic activity for E. coli disinfection and organic pollutant degradation. Journal of Colloid and Interface Science, 2018, 512, 555-566.	5.0	84
84	Bismuth-rich bismuth oxyhalides: a new opportunity to trigger high-efficiency photocatalysis. Journal of Materials Chemistry A, 2020, 8, 21434-21454.	5.2	84
85	Harnessing strong metal–support interactions via a reverse route. Nature Communications, 2020, 11, 3042.	5.8	84
86	Mo-O-Bi Bonds as interfacial electron transport bridges to fuel CO2 photoreduction via in-situ reconstruction of black Bi2MoO6/BiO2-x heterojunction. Chemical Engineering Journal, 2022, 429, 132204.	6.6	83
87	Interfacial chemical bond modulated Bi19S27Br3/g-C3N4 Z-scheme heterojunction for enhanced photocatalytic CO2 conversion. Applied Catalysis B: Environmental, 2022, 307, 121162.	10.8	83
88	Strain-Engineering of Bi ₁₂ O ₁₇ Br ₂ Nanotubes for Boosting Photocatalytic CO ₂ Reduction. , 2020, 2, 1025-1032.		82
89	Fenton-like ionic liquids/H ₂ O ₂ system: one-pot extraction combined with oxidation desulfurization of fuel. RSC Advances, 2012, 2, 658-664.	1.7	81
90	Theoretical evidence of charge transfer interaction between SO ₂ and deep eutectic solvents formed by choline chloride and glycerol. Physical Chemistry Chemical Physics, 2015, 17, 28729-28742.	1.3	80

#	Article	IF	CITATIONS
91	An Allâ€Organic Dâ€A System for Visible‣ightâ€Driven Overall Water Splitting. Small, 2020, 16, e2003914.	5.2	80
92	Synthesis of Ionic-Liquid-Based Deep Eutectic Solvents for Extractive Desulfurization of Fuel. Energy & Fuels, 2016, 30, 8164-8170.	2.5	79
93	A large number of low coordinated atoms in boron nitride for outstanding adsorptive desulfurization performance. Green Chemistry, 2016, 18, 3040-3047.	4.6	79
94	Nonâ€Covalent Interaction of Atomically Dispersed Cu and Zn Pair Sites for Efficient Oxygen Reduction Reaction. Advanced Functional Materials, 2022, 32, .	7.8	79
95	Graphene quantum dots modified flower like Bi2WO6 for enhanced photocatalytic nitrogen fixation. Journal of Colloid and Interface Science, 2019, 557, 498-505.	5.0	78
96	Achieving Ultrahigh Capacity with Self-Assembled Ni(OH) ₂ Nanosheet-Decorated Hierarchical Flower-like MnCo ₂ O _{4.5} Nanoneedles as Advanced Electrodes of Battery–Supercapacitor Hybrid Devices. ACS Applied Materials & Interfaces, 2019, 11, 9984-9993.	4.0	78
97	Enhanced Oxygen Activation Achieved by Robust Single Chromium Atom-Derived Catalysts in Aerobic Oxidative Desulfurization. ACS Catalysis, 2022, 12, 8623-8631.	5.5	78
98	Synthesis and characterization of g-C ₃ N ₄ /Ag ₂ CO ₃ with enhanced visible-light photocatalytic activity for the degradation of organic pollutants. RSC Advances, 2014, 4, 34539.	1.7	77
99	Oxygen vacancies modulated Bi-rich bismuth oxyiodide microspheres with tunable valence band position to boost the photocatalytic activity. Journal of Colloid and Interface Science, 2019, 533, 612-620.	5.0	77
100	Plasma treated Bi ₂ WO ₆ ultrathin nanosheets with oxygen vacancies for improved photocatalytic CO ₂ reduction. Inorganic Chemistry Frontiers, 2020, 7, 597-602.	3.0	77
101	Revealing the role of oxygen vacancies in bimetallic PbBiO2Br atomic layers for boosting photocatalytic CO2 conversion. Applied Catalysis B: Environmental, 2020, 277, 119170.	10.8	77
102	Synthesis and photocatalytic activity of a bentonite/g-C3N4 composite. RSC Advances, 2014, 4, 11831.	1.7	76
103	A Specifically Exposed Cobalt Oxide/Carbon Nitride 2D Heterostructure for Carbon Dioxide Photoreduction. Industrial & Engineering Chemistry Research, 2018, 57, 17394-17400.	1.8	76
104	The CoMo-LDH ultrathin nanosheet as a highly active and bifunctional electrocatalyst for overall water splitting. Inorganic Chemistry Frontiers, 2018, 5, 2964-2970.	3.0	76
105	Taming Interfacial Oxygen Vacancies of Amphiphilic Tungsten Oxide for Enhanced Catalysis in Oxidative Desulfurization. ACS Sustainable Chemistry and Engineering, 2017, 5, 8930-8938.	3.2	75
106	Confined active species and effective charge separation in Bi4O5I2 ultrathin hollow nanotube with increased photocatalytic activity. Applied Catalysis B: Environmental, 2020, 268, 118403.	10.8	75
107	Non-metal photocatalyst nitrogen-doped carbon nanotubes modified mpg-C3N4: facile synthesis and the enhanced visible-light photocatalytic activity. Journal of Colloid and Interface Science, 2017, 494, 38-46.	5.0	74
108	Magnetically controlled fluorescence aptasensor for simultaneous determination of ochratoxin A and aflatoxin B1. Analytica Chimica Acta, 2018, 1019, 119-127.	2.6	74

#	Article	IF	CITATIONS
109	Hydrothermal synthesis of mpg-C ₃ N ₄ and Bi ₂ WO ₆ nest-like structure nanohybrids with enhanced visible light photocatalytic activities. RSC Advances, 2017, 7, 38682-38690.	1.7	73
110	Synthesis of mesoporous WO ₃ /TiO ₂ catalyst and its excellent catalytic performance for the oxidation of dibenzothiophene. New Journal of Chemistry, 2017, 41, 569-578.	1.4	72
111	Polyoxometalate-Based Poly(ionic liquid) as a Precursor for Superhydrophobic Magnetic Carbon Composite Catalysts toward Aerobic Oxidative Desulfurization. ACS Sustainable Chemistry and Engineering, 2019, 7, 15755-15761.	3.2	72
112	Silver Nanoparticle-Decorated Boron Nitride with Tunable Electronic Properties for Enhancement of Adsorption Performance. ACS Sustainable Chemistry and Engineering, 2018, 6, 4948-4957.	3.2	71
113	Non-covalent modification of graphene oxide nanocomposites with chitosan/dextran and its application in drug delivery. RSC Advances, 2016, 6, 9328-9337.	1.7	69
114	Insight into the Potassium Poisoning Effect for Selective Catalytic Reduction of NO _{<i>x</i>} with NH ₃ over Fe/Beta. ACS Catalysis, 2021, 11, 14727-14739.	5.5	69
115	A multidimensional In ₂ S ₃ –CuInS ₂ heterostructure for photocatalytic carbon dioxide reduction. Inorganic Chemistry Frontiers, 2018, 5, 3163-3169.	3.0	67
116	Single-metal-atom catalysts: An emerging platform for electrocatalytic oxygen reduction. Chemical Engineering Journal, 2021, 406, 127135.	6.6	67
117	Solvothermal synthesis and enhanced visible-light photocatalytic decontamination of bisphenol A (BPA) by g-C3N4/BiOBr heterojunctions. Materials Science in Semiconductor Processing, 2014, 24, 96-103.	1.9	66
118	Ionic liquid-induced double regulation of carbon quantum dots modified bismuth oxychloride/bismuth oxybromide nanosheets with enhanced visible-light photocatalytic activity. Journal of Colloid and Interface Science, 2018, 519, 263-272.	5.0	66
119	Ionic liquid-assisted synthesis and improved photocatalytic activity of p-n junction g-C3N4/BiOCl. Journal of Materials Science, 2016, 51, 4769-4777.	1.7	65
120	Controllable Fabrication of Tungsten Oxide Nanoparticles Confined in Grapheneâ€Analogous Boron Nitride as an Efficient Desulfurization Catalyst. Chemistry - A European Journal, 2015, 21, 15421-15427.	1.7	63
121	Graphitic carbon nitride/BiOCl composites for sensitive photoelectrochemical detection of ciprofloxacin. Journal of Colloid and Interface Science, 2016, 483, 241-248.	5.0	63
122	Hexamethylenetetramine-assisted hydrothermal synthesis of octahedral nickel ferrite oxide nanocrystallines with excellent supercapacitive performance. Journal of Materials Science, 2018, 53, 7621-7636.	1.7	63
123	MnCo ₂ S ₄ /FeCo ₂ S ₄ "lollipop―arrays on a hollow N-doped carbon skeleton as flexible electrodes for hybrid supercapacitors. Journal of Materials Chemistry A, 2019, 7, 20778-20789.	5.2	63
124	Photocatalytic oxidative desulfurization of dibenzothiophene catalyzed by amorphous TiO2 in ionic liquid. Korean Journal of Chemical Engineering, 2014, 31, 211-217.	1.2	62
125	Graphene-Analogues Boron Nitride Nanosheets Confining Ionic Liquids: A High-Performance Quasi-Liquid Solid Electrolyte. Small, 2016, 12, 3535-3542.	5.2	62
126	An Fe-doped NiV LDH ultrathin nanosheet as a highly efficient electrocatalyst for efficient water oxidation. Inorganic Chemistry Frontiers, 2019, 6, 1890-1896.	3.0	61

#	Article	IF	CITATIONS
127	In situ construction efficient visible-light-driven three-dimensional Polypyrrole/Zn3In2S6 nanoflower to systematically explore the photoreduction of Cr(VI): Performance, factors and mechanism. Journal of Hazardous Materials, 2020, 384, 121480.	6.5	61
128	Selenium-rich nickel cobalt bimetallic selenides with core–shell architecture enable superior hybrid energy storage devices. Nanoscale, 2020, 12, 4040-4050.	2.8	61
129	Tailoring Nâ€Terminated Defective Edges of Porous Boron Nitride for Enhanced Aerobic Catalysis. Small, 2017, 13, 1701857.	5.2	60
130	Highly efficient phenothiazine 5,5-dioxide-based hole transport materials for planar perovskite solar cells with a PCE exceeding 20%. Journal of Materials Chemistry A, 2019, 7, 9510-9516.	5.2	60
131	Immobilizing Highly Catalytically Molybdenum Oxide Nanoparticles on Graphene-Analogous BN: Stable Heterogeneous Catalysts with Enhanced Aerobic Oxidative Desulfurization Performance. Industrial & Engineering Chemistry Research, 2019, 58, 863-871.	1.8	60
132	Graphene-like boron nitride modified bismuth phosphate materials for boosting photocatalytic degradation of enrofloxacin. Journal of Colloid and Interface Science, 2017, 492, 51-60.	5.0	59
133	Construction of SnO ₂ /graphene-like g-C ₃ N ₄ with enhanced visible light photocatalytic activity. RSC Advances, 2017, 7, 36101-36111.	1.7	59
134	Efficient Synthesis of 1-Acetylpyrene Using [Bmim]Cl–FeCl3 Ionic Liquid as Dual Catalyst and Solvent. International Journal of Chemical Reactor Engineering, 2013, 11, 1-7.	0.6	58
135	Synthesis and photocatalytic activity of g-C ₃ N ₄ /BiOI/BiOBr ternary composites. RSC Advances, 2016, 6, 41204-41213.	1.7	58
136	Low cost and green preparation process for α-Fe ₂ O ₃ @gum arabic electrode for high performance sodium ion batteries. Journal of Materials Chemistry A, 2017, 5, 2102-2109.	5.2	58
137	Synthesis of zinc ferrite/silver iodide composite with enhanced photocatalytic antibacterial and pollutant degradation ability. Journal of Colloid and Interface Science, 2018, 528, 70-81.	5.0	58
138	Highâ€performance adsorptive desulfurization by ternary hybrid boron carbon nitride aerogel. AICHE Journal, 2021, 67, e17280.	1.8	58
139	Immobilized fentonâ€like ionic liquid: Catalytic performance for oxidative desulfurization. AICHE Journal, 2013, 59, 4696-4704.	1.8	57
140	Microwave-assisted synthesis of few-layered MoS2/BiOBr hollow microspheres with superior visible-light-response photocatalytic activity for ciprofloxacin removal. CrystEngComm, 2015, 17, 3645-3651.	1.3	57
141	Magnetically separable Fe2O3/g-C3N4 catalyst with enhanced photocatalytic activity. RSC Advances, 2015, 5, 95727-95735.	1.7	57
142	Accelerating Photogenerated Charge Kinetics via the Synergetic Utilization of 2D Semiconducting Structural Advantages and Nobleâ€Metalâ€Free Schottky Junction Effect. Small, 2019, 15, e1804613.	5.2	56
143	Low-crystalline mesoporous CoFe ₂ O ₄ /C composite with oxygen vacancies for high energy density asymmetric supercapacitors. RSC Advances, 2017, 7, 55513-55522.	1.7	55
144	Construction of oxygen vacancy assisted Z-scheme BiO2â°'x/BiOBr heterojunction for LED light pollutants degradation and bacteria inactivation. Journal of Colloid and Interface Science, 2021, 600, 344-357.	5.0	55

#	Article	IF	CITATIONS
145	Atomically Thin 2D Multinary Nanosheets for Energyâ€Related Photo, Electrocatalysis. Advanced Science, 2018, 5, 1800244.	5.6	54
146	Novel Z-scheme heterogeneous photo-Fenton-like g-C3N4/FeOCl for the pollutants degradation under visible light irradiation. Journal of Photochemistry and Photobiology A: Chemistry, 2020, 391, 112343.	2.0	54
147	Green aqueous biphasic systems containing deep eutectic solvents and sodium salts for the extraction of protein. RSC Advances, 2017, 7, 49361-49367.	1.7	53
148	Enhanced long-wavelength light utilization with polyaniline/bismuth-rich bismuth oxyhalide composite towards photocatalytic degradation of antibiotics. Journal of Colloid and Interface Science, 2019, 537, 101-111.	5.0	53
149	Nitrogen-rich graphitic carbon nitride nanotubes for photocatalytic hydrogen evolution with simultaneous contaminant degradation. Journal of Colloid and Interface Science, 2020, 560, 555-564.	5.0	53
150	A Janus cobalt nanoparticles and molybdenum carbide decorated N-doped carbon for high-performance overall water splitting. Journal of Colloid and Interface Science, 2021, 583, 614-625.	5.0	53
151	Hydrophobic mesoporous silica-supported heteropolyacid induced by ionic liquid as a high efficiency catalyst for the oxidative desulfurization of fuel. RSC Advances, 2015, 5, 16847-16855.	1.7	52
152	Graphitic Carbon Nitride Nanorods for Photoelectrochemical Sensing of Trace Copper(II) Ions. European Journal of Inorganic Chemistry, 2014, 2014, 3665-3673.	1.0	51
153	High yield synthesis of nano-size g-C ₃ N ₄ derivatives by a dissolve-regrowth method with enhanced photocatalytic ability. RSC Advances, 2015, 5, 26281-26290.	1.7	51
154	Ionic liquid-assisted bidirectional regulation strategy for carbon quantum dots (CQDs)/Bi4O5I2 nanomaterials and enhanced photocatalytic properties. Journal of Colloid and Interface Science, 2016, 478, 324-333.	5.0	51
155	A simple and cost-effective extractive desulfurization process with novel deep eutectic solvents. RSC Advances, 2016, 6, 30345-30352.	1.7	51
156	Metalâ€free boron nitride adsorbent for ultraâ€deep desulfurization. AICHE Journal, 2017, 63, 3463-3469.	1.8	51
157	Magnetically Separable Fe3O4 Nanoparticles-Decorated Reduced Graphene Oxide Nanocomposite for Catalytic Wet Hydrogen Peroxide Oxidation. Journal of Inorganic and Organometallic Polymers and Materials, 2013, 23, 907-916.	1.9	50
158	The enhanced visible light photocatalytic activity of yttrium-doped BiOBr synthesized via a reactable ionic liquid. Applied Surface Science, 2015, 331, 170-178.	3.1	50
159	g < ₃ N ₄ /TiO ₂ Nanocomposites for Degradation of Ciprofloxacin under Visible Light Irradiation. ChemistrySelect, 2016, 1, 5679-5685.	0.7	50
160	Carbonized polymer dots modified ultrathin Bi12O17Cl2 nanosheets Z-scheme heterojunction for robust CO2 photoreduction. Chemical Engineering Science, 2021, 232, 116338.	1.9	48
161	Design of Lewis Acid Centers in Bundlelike Boron Nitride for Boosting Adsorptive Desulfurization Performance. Industrial & Engineering Chemistry Research, 2019, 58, 13303-13312.	1.8	47
162	Accelerated Photoreduction of CO ₂ to CO over a Stable Heterostructure with a Seamless Interface. ACS Applied Materials & Interfaces, 2021, 13, 39523-39532.	4.0	47

#	Article	IF	CITATIONS
163	Anchoring Copper Single Atoms on Porous Boron Nitride Nanofiber to Boost Selective Reduction of Nitroaromatics. ACS Nano, 2022, 16, 4152-4161.	7.3	47
164	Supported ionic liquid [Bmim]FeCl ₄ /Am TiO ₂ as an efficient catalyst for the catalytic oxidative desulfurization of fuels. RSC Advances, 2015, 5, 43528-43536.	1.7	45
165	Molybdenum-containing dendritic mesoporous silica spheres for fast oxidative desulfurization in fuel. Inorganic Chemistry Frontiers, 2019, 6, 451-458.	3.0	45
166	Partially etched Bi2O2CO3 by metal chloride for enhanced reactive oxygen species generation: A tale of two strategies. Applied Catalysis B: Environmental, 2019, 245, 325-333.	10.8	45
167	Macroporous polystyrene resins as adsorbents for the removal of tetracycline antibiotics from an aquatic environment. Journal of Applied Polymer Science, 2014, 131, .	1.3	44
168	Controlled Gas Exfoliation of Boron Nitride into Few‣ayered Nanosheets. Angewandte Chemie, 2016, 128, 10924-10928.	1.6	44
169	Efficient photocatalytic hydrogen evolution mediated by defect-rich 1T-PtS ₂ atomic layer nanosheet modified mesoporous graphitic carbon nitride. Journal of Materials Chemistry A, 2019, 7, 18906-18914.	5.2	44
170	Charge steering in ultrathin 2D nanomaterials for photocatalysis. Journal of Materials Chemistry A, 2020, 8, 12928-12950.	5.2	44
171	Ion-exchange preparation for visible-light-driven photocatalyst AgBr/Ag2CO3 and its photocatalytic activity. RSC Advances, 2014, 4, 9139.	1.7	43
172	Ionic liquid-assisted strategy for bismuth-rich bismuth oxybromides nanosheets with superior visible light-driven photocatalytic removal of bisphenol-A. Journal of Colloid and Interface Science, 2016, 473, 112-119.	5.0	43
173	TiO ₂ microspheres supported polyoxometalate-based ionic liquids induced catalytic oxidative deep-desulfurization. RSC Advances, 2016, 6, 42402-42412.	1.7	43
174	Novel Ag ₂ S quantum dot modified 3D flower-like SnS ₂ composites for photocatalytic and photoelectrochemical applications. Inorganic Chemistry Frontiers, 2018, 5, 63-72.	3.0	43
175	Construction of NH2-MIL-125(Ti)/Bi2WO6 composites with accelerated charge separation for degradation of organic contaminants under visible light irradiation. Green Energy and Environment, 2020, 5, 203-213.	4.7	43
176	An efficient broad spectrum-driven carbon and oxygen co-doped g-C3N4 for the photodegradation of endocrine disrupting: Mechanism, degradation pathway, DFT calculation and toluene selective oxidation. Journal of Hazardous Materials, 2021, 401, 123309.	6.5	43
177	O ₂ Activation and Oxidative Dehydrogenation of Propane on Hexagonal Boron Nitride: Mechanism Revisited. Journal of Physical Chemistry C, 2019, 123, 2256-2266.	1.5	42
178	Oxygen Vacancies Engineering–Mediated BiOBr Atomic Layers for Boosting Visible Lightâ€Đriven Photocatalytic CO ₂ Reduction. Solar Rrl, 2021, 5, 2000480.	3.1	42
179	Photocatalytic degradation of methylene blue on magnetically separable FePc/Fe3O4 nanocomposite under visible irradiation. Pure and Applied Chemistry, 2009, 81, 2327-2335.	0.9	41
180	Synthesis and characterization of BN/Bi ₂ WO ₆ composite photocatalysts with enhanced visible-light photocatalytic activity. RSC Advances, 2015, 5, 88832-88840.	1.7	41

#	Article	IF	CITATIONS
181	A core–shell structured magnetic Ag/AgBr@Fe ₂ O ₃ composite with enhanced photocatalytic activity for organic pollutant degradation and antibacterium. RSC Advances, 2015, 5, 71035-71045.	1.7	41
182	Highly Efficient Phenoxazine Core Unit Based Hole Transport Materials for Hysteresis-Free Perovskite Solar Cells. ACS Applied Materials & Interfaces, 2018, 10, 36608-36614.	4.0	41
183	In-situ preparation of MIL-125(Ti)/Bi2WO6 photocatalyst with accelerating charge carriers for the photodegradation of tetracycline hydrochloride. Journal of Photochemistry and Photobiology A: Chemistry, 2020, 387, 112149.	2.0	41
184	Mechanical exfoliation of boron carbide: A metal-free catalyst for aerobic oxidative desulfurization in fuel. Journal of Hazardous Materials, 2020, 391, 122183.	6.5	41
185	Photoelectrochemical sensing of 4-chlorophenol based on Au/BiOCl nanocomposites. Talanta, 2016, 156-157, 257-264.	2.9	40
186	A Z-scheme magnetic recyclable Ag/AgBr@CoFe ₂ O ₄ photocatalyst with enhanced photocatalytic performance for pollutant and bacterial elimination. RSC Advances, 2017, 7, 30845-30854.	1.7	40
187	One-pot extraction and aerobic oxidative desulfurization with highly dispersed V ₂ O ₅ /SBA-15 catalyst in ionic liquids. RSC Advances, 2017, 7, 39383-39390.	1.7	40
188	Atomic-level active sites steering in ultrathin photocatalysts to trigger high efficiency nitrogen fixation. Chemical Engineering Journal, 2020, 402, 126208.	6.6	40
189	Graphene-like BN@SiO2 nanocomposites as efficient sorbents for solid-phase extraction of Rhodamine B and Rhodamine 6G from food samples. Food Chemistry, 2020, 320, 126666.	4.2	40
190	Oxygen vacancies in Bi2Sn2O7 quantum dots to trigger efficient photocatalytic nitrogen reduction. Applied Catalysis B: Environmental, 2021, 299, 120680.	10.8	40
191	Few‣ayer Boron Nitride with Engineered Nitrogen Vacancies for Promoting Conversion of Polysulfide as a Cathode Matrix for Lithium–Sulfur Batteries. Chemistry - A European Journal, 2019, 25, 8112-8117.	1.7	39
192	Porous defective carbon nitride obtained by a universal method for photocatalytic hydrogen production from water splitting. Journal of Colloid and Interface Science, 2020, 566, 171-182.	5.0	39
193	Polyoxometalate@magnetic graphene as versatile immobilization matrix of Ru(bpy)32+ for sensitive magneto-controlled electrochemiluminescence sensor and its application in biosensing. Biosensors and Bioelectronics, 2014, 57, 149-156.	5.3	38
194	Controlled preparation of MoS2/PbBiO2I hybrid microspheres with enhanced visible-light photocatalytic behaviour. Journal of Colloid and Interface Science, 2018, 517, 278-287.	5.0	38
195	Defectâ€Rich Bi ₁₂ O ₁₇ Cl ₂ Nanotubes Selfâ€Accelerating Charge Separation for Boosting Photocatalytic CO ₂ Reduction. Angewandte Chemie, 2018, 130, 15063-15067.	1.6	38
196	Ionic liquid-supported 3DOM silica for efficient heterogeneous oxidative desulfurization. Inorganic Chemistry Frontiers, 2018, 5, 2478-2485.	3.0	38
197	Scalable Synthesis of Micromesoporous Iron-Nitrogen-Doped Carbon as Highly Active and Stable Oxygen Reduction Electrocatalyst. ACS Applied Materials & Interfaces, 2019, 11, 39263-39273.	4.0	38
198	Constructing a CeO _{2â~'x} @CoFe-layered double hydroxide heterostructure as an improved electrocatalyst for highly efficient water oxidation. Inorganic Chemistry Frontiers, 2020, 7, 4461-4468.	3.0	38

#	Article	IF	CITATIONS
199	Amorphous TiO ₂ â€Derived Largeâ€Capacity Lithium Ion Sieve for Lithium Recovery. Chemical Engineering and Technology, 2020, 43, 1784-1791.	0.9	38
200	Unique Dual‣ites Boosting Overall CO ₂ Photoconversion by Hierarchical Electron Harvesters. Small, 2021, 17, e2103796.	5.2	38
201	One-dimensional β-Ni(OH)2 nanostructures: Ionic liquid etching synthesis, formation mechanism, and application for electrochemical capacitors. CrystEngComm, 2011, 13, 7108.	1.3	37
202	Modification of Ag ₃ VO ₄ with graphene-like MoS ₂ for enhanced visible-light photocatalytic property and stability. New Journal of Chemistry, 2016, 40, 2168-2177.	1.4	37
203	Tuning electronic properties of boron nitride nanoplate via doping carbon for enhanced adsorptive performance. Journal of Colloid and Interface Science, 2017, 508, 121-128.	5.0	37
204	Metallic cobalt nanoparticles embedded in sulfur and nitrogen co-doped rambutan-like nanocarbons for the oxygen reduction reaction under both acidic and alkaline conditions. Journal of Materials Chemistry A, 2019, 7, 14291-14301.	5.2	37
205	Aerobic Oxidative Desulfurization by Nanoporous Tungsten Oxide with Oxygen Defects. ACS Applied Nano Materials, 2021, 4, 1085-1093.	2.4	37
206	Graphene-analogue boron nitride/Ag ₃ PO ₄ composite for efficient visible-light-driven photocatalysis. RSC Advances, 2014, 4, 56853-56862.	1.7	36
207	Chemical reduction implanted oxygen vacancy on the surface of 1D MoO3â^'x/g-C3N4 composite for boosted LED light-driven photoactivity. Journal of Materials Science, 2019, 54, 5343-5358.	1.7	36
208	Novel broad-spectrum-driven oxygen-linked band and porous defect co-modified orange carbon nitride for photodegradation of Bisphenol A and 2-Mercaptobenzothiazole. Journal of Hazardous Materials, 2020, 396, 122659.	6.5	36
209	Development of novel graphene-like layered hexagonal boron nitride for adsorptive removal of antibiotic gatifloxacin from aqueous solution. Green Chemistry Letters and Reviews, 2014, 7, 330-336.	2.1	35
210	Ag ₂ S quantum dots in situ coupled to hexagonal SnS ₂ with enhanced photocatalytic activity for MO and Cr(<scp>vi</scp>) removal. RSC Advances, 2017, 7, 46823-46831.	1.7	35
211	Synthesis of WO3/mesoporous ZrO2 catalyst as a high-efficiency catalyst for catalytic oxidation of dibenzothiophene in diesel. Journal of Materials Science, 2018, 53, 15927-15938.	1.7	35
212	Highly Efficient Visible-Light-Driven Schottky Catalyst MoN/2D g-C ₃ N ₄ for Hydrogen Production and Organic Pollutants Degradation. Industrial & Engineering Chemistry Research, 2018, 57, 8863-8870.	1.8	35
213	Construction of ultrathin MoS2/Bi5O7I composites: Effective charge separation and increased photocatalytic activity. Journal of Colloid and Interface Science, 2020, 560, 475-484.	5.0	35
214	Theoretical investigation of the interaction between aromatic sulfur compounds and [BMIM]+[FeCl4]â^' ionic liquid in desulfurization: A novel charge transfer mechanism. Journal of Molecular Graphics and Modelling, 2015, 59, 40-49.	1.3	34
215	Enhanced reactive oxygen species activation for building carbon quantum dots modified Bi5O7I nanorod composites and optimized visible-light-response photocatalytic performance. Journal of Colloid and Interface Science, 2018, 532, 727-737.	5.0	34
216	Macroscopic 3D boron nitride monolith for efficient adsorptive desulfurization. Fuel, 2020, 261, 116448.	3.4	34

#	Article	IF	CITATIONS
217	Manganeseâ€Modulated Cobaltâ€Based Layered Double Hydroxide Grown on Nickel Foam with 1D–2D–3D Heterostructure for Highly Efficient Oxygen Evolution Reaction and Urea Oxidation Reaction. Chemistry - A European Journal, 2020, 26, 9382-9388.	1.7	34
218	Construction of single-atom catalysts for electro-, photo- and photoelectro-catalytic applications: State-of-the-art, opportunities, and challenges. Materials Today, 2022, 53, 217-237.	8.3	34
219	Deep oxidative desulfurization of fuels catalyzed by magnetic Fenton-like hybrid catalysts in ionic liquids. RSC Advances, 2013, 3, 2355.	1.7	33
220	Designing multifunctional SO ₃ H-based polyoxometalate catalysts for oxidative desulfurization in acid deep eutectic solvents. RSC Advances, 2017, 7, 55318-55325.	1.7	33
221	Dispersing TiO ₂ Nanoparticles on Graphite Carbon for an Enhanced Catalytic Oxidative Desulfurization Performance. Industrial & Engineering Chemistry Research, 2020, 59, 18471-18479.	1.8	33
222	Preparation of magnetic Ag/AgCl/CoFe ₂ O ₄ composites with high photocatalytic and antibacterial ability. RSC Advances, 2015, 5, 41475-41483.	1.7	32
223	Core–shell magnetic Ag/AgCl@Fe ₂ O ₃ photocatalysts with enhanced photoactivity for eliminating bisphenol A and microbial contamination. New Journal of Chemistry, 2016, 40, 3413-3422.	1.4	32
224	In-situ preparation of iron(II) phthalocyanine modified bismuth oxybromide with enhanced visible-light photocatalytic activity and mechanism insight. Colloids and Surfaces A: Physicochemical and Engineering Aspects, 2019, 575, 336-345.	2.3	32
225	Ionic liquid induced mechanochemical synthesis of BiOBr ultrathin nanosheets at ambient temperature with superior visible-light-driven photocatalysis. Journal of Colloid and Interface Science, 2020, 574, 131-139.	5.0	32
226	Interface engineering in low-dimensional bismuth-based materials for photoreduction reactions. Journal of Materials Chemistry A, 2021, 9, 2662-2677.	5.2	32
227	Selective adsorption and degradation of rhodamine B with modified titanium dioxide photocatalyst. Journal of Applied Polymer Science, 2014, 131, .	1.3	31
228	Design of 3D WO ₃ /h-BN nanocomposites for efficient visible-light-driven photocatalysis. RSC Advances, 2017, 7, 25160-25170.	1.7	31
229	Novel mesoporous graphitic carbon nitride modified PbBiO2Br porous microspheres with enhanced photocatalytic performance. Journal of Colloid and Interface Science, 2017, 507, 310-322.	5.0	31
230	NiMoO ₄ nanorod deposited carbon sponges with ant-nest-like interior channels for high-performance pseudocapacitors. Inorganic Chemistry Frontiers, 2018, 5, 1594-1601.	3.0	31
231	Graphene oxide-modified LaVO ₄ nanocomposites with enhanced photocatalytic degradation efficiency of antibiotics. Inorganic Chemistry Frontiers, 2018, 5, 2818-2828.	3.0	31
232	Porous Nb ₄ N ₅ /rGO Nanocomposite for Ultrahigh-Energy-Density Lithium-Ion Hybrid Capacitor. ACS Applied Materials & Interfaces, 2019, 11, 24114-24121.	4.0	31
233	Commercial Diatomite for Adsorption of Tetracycline Antibiotic from Aqueous Solution. Separation Science and Technology, 2014, 49, 2221-2227.	1.3	30
234	Fabrication of magnetic BaFe ₁₂ O ₁₉ /Ag ₃ PO ₄ composites with an <i>in situ</i> photo-Fenton-like reaction for enhancing reactive oxygen species under visible light irradiation. Catalysis Science and Technology, 2019, 9, 2563-2570.	2.1	30

#	Article	IF	CITATIONS
235	Atomic-Layered α-V ₂ O ₅ Nanosheets Obtained via Fast Gas-Driven Exfoliation for Superior Aerobic Oxidative Desulfurization. Energy & Fuels, 2020, 34, 2612-2616.	2.5	30
236	Fast Oxidative Removal of Refractory Aromatic Sulfur Compounds by a Magnetic Ionic Liquid. Chemical Engineering and Technology, 2014, 37, 36-42.	0.9	29
237	Glucose dehydration to 5-hydroxymethylfurfural in ionic liquid over Cr ³⁺ -modified ion exchange resin. RSC Advances, 2015, 5, 9290-9297.	1.7	29
238	Plasma-induced defect engineering: Boosted the reverse water gas shift reaction performance with electron trap. Journal of Colloid and Interface Science, 2020, 580, 814-821.	5.0	29
239	MO degradation by Ag–Ag2O/g-C3N4 composites under visible-light irradation. SpringerPlus, 2016, 5, 369.	1.2	28
240	Novel visible-light-driven Fe ₂ O ₃ /Ag ₃ VO ₄ composite with enhanced photocatalytic activity toward organic pollutants degradation. RSC Advances, 2016, 6, 3600-3607.	1.7	28
241	Controllable synthesis of perovskite-like PbBiO ₂ Cl hollow microspheres with enhanced photocatalytic activity for antibiotic removal. CrystEngComm, 2017, 19, 4777-4788.	1.3	28
242	Multiple Active Sites of Carbon for Highâ€Rate Surface apacitive Sodiumâ€Ion Storage. Angewandte Chemie, 2019, 131, 13718-13723.	1.6	28
243	High-performance electrolytic oxygen evolution with a seamless armor core–shell FeCoNi oxynitride. Nanoscale, 2019, 11, 7239-7246.	2.8	28
244	Accelerating the Hole Mobility of Graphitic Carbon Nitride for Photocatalytic Hydrogen Evolution via 2D/2D Heterojunction Structural Advantages and Ni(OH) ₂ Characteristic. Solar Rrl, 2020, 4, 1900538.	3.1	28
245	Application of a self-emulsifiable task-specific ionic liquid in oxidative desulfurization of fuels. RSC Advances, 2013, 3, 3893.	1.7	27
246	Grapheneâ€analogue molybdenum disulfide for adsorptive removal of tetracycline from aqueous solution: equilibrium, kinetic, and thermodynamic studies. Environmental Progress and Sustainable Energy, 2017, 36, 815-821.	1.3	27
247	Two-Dimensional Mn-Co LDH/Graphene Composite towards High-Performance Water Splitting. Catalysts, 2018, 8, 350.	1.6	27
248	Single Transition Metal Atom-Doped Graphene Supported on a Nickel Substrate: Enhanced Oxygen Reduction Reactions Modulated by Electron Coupling. Journal of Physical Chemistry C, 2019, 123, 3703-3710.	1.5	27
249	The novel photo-Fenton-like few-layer MoS2/FeVO4 composite for improved degradation activity under visible light irradiation. Colloids and Surfaces A: Physicochemical and Engineering Aspects, 2021, 623, 126721.	2.3	27
250	Edgeâ€ S iteâ€Rich Ordered Macroporous BiOCl Triggers CO Activation for Efficient CO ₂ Photoreduction. Small, 2022, 18, e2105228.	5.2	27
251	Universal strategy engineering grain boundaries for catalytic oxidative desulfurization. Applied Catalysis B: Environmental, 2022, 317, 121714.	10.8	27
252	Phosphomolybdic acid immobilized on ionic liquid-modified hexagonal boron nitride for oxidative desulfurization of fuel. RSC Advances, 2017, 7, 54266-54276.	1.7	26

#	Article	IF	CITATIONS
253	Advanced Overlap Adsorption Model of Few-Layer Boron Nitride for Aromatic Organic Pollutants. Industrial & Engineering Chemistry Research, 2018, 57, 4045-4051.	1.8	26
254	Realizing the synergistic effect of electronic modulation over graphitic carbon nitride for highly efficient photodegradation of bisphenol A and 2-mercaptobenzothiazole: Mechanism, degradation pathway and density functional theory calculation. Journal of Colloid and Interface Science, 2021, 583, 113-127.	5.0	26
255	An accurate empirical method to predict the adsorption strength for ï€-orbital contained molecules on two dimensional materials. Journal of Molecular Graphics and Modelling, 2018, 82, 93-100.	1.3	25
256	Catalytic oxidative desulfurization of fuels in acidic deep eutectic solvents with [(C6H13)3P(C14H29)]3PMo12O40 as a catalyst. Petroleum Science, 2018, 15, 841-848.	2.4	25
257	Exploitation of a photoelectrochemical sensing platform for catechol quantitative determination using BiPO4 nanocrystals/BiOI heterojunction. Analytica Chimica Acta, 2018, 1042, 11-19.	2.6	25
258	Synthesis of N,O-Doped Porous Graphene from Petroleum Coke for Deep Oxidative Desulfurization of Fuel. Energy & Fuels, 2019, 33, 8302-8311.	2.5	25
259	Graphene Oxide-Loaded SnO ₂ Quantum Wires with Sub-4 Nanometer Diameters for Low-Temperature H ₂ S Gas Sensing. ACS Applied Nano Materials, 2020, 3, 6385-6393.	2.4	25
260	Oxygenâ€Defective TiNb ₂ O _{7â€} <i>_x</i> Nanochains with Enlarged Lattice Spacing for Highâ€Rate Lithium Ion Capacitor. Advanced Materials Interfaces, 2020, 7, 2000705.	1.9	25
261	The CeO ₂ /Ag ₃ PO ₄ photocatalyst with stability and high photocatalyst activity under visible light irradiation. Physica Status Solidi (A) Applications and Materials Science, 2016, 213, 2356-2363.	0.8	24
262	Hierarchical FeCo ₂ S ₄ Nanotube Arrays Deposited on 3D Carbon Foam as Binderâ€free Electrodes for Highâ€performance Asymmetric Pseudocapacitors. Chemistry - an Asian Journal, 2018, 13, 3212-3221.	1.7	24
263	Structure and catalytic oxidative desulfurization properties of SBA-15 supported silicotungstic acid ionic liquid. Journal of Porous Materials, 2016, 23, 823-831.	1.3	23
264	Facile synthesis of CNT/AgI with enhanced photocatalytic degradation and antibacterial ability. RSC Advances, 2016, 6, 6905-6914.	1.7	23
265	Photoelectrochemical sensing of bisphenol a based on graphitic carbon nitride/bismuth oxyiodine composites. RSC Advances, 2017, 7, 7929-7935.	1.7	23
266	Preparation of oxygen-deficient 2D WO3â^'x nanoplates and their adsorption behaviors for organic pollutants: equilibrium and kinetics modeling. Journal of Materials Science, 2019, 54, 12463-12475.	1.7	23
267	A composite prepared from BiOBr and gold nanoparticles with electron sink and hot-electron donor properties for photoelectrochemical aptasensing of tetracycline. Mikrochimica Acta, 2019, 186, 794.	2.5	23
268	Heterogenization of homogenous oxidative desulfurization reaction on graphene-like boron nitride with a peroxomolybdate ionic liquid. RSC Advances, 2016, 6, 140-147.	1.7	22
269	Construction of solid–liquid interfacial Fenton-like reaction under visible light irradiation over etched CoxFeyO4–BiOBr photocatalysts. Catalysis Science and Technology, 2018, 8, 551-561.	2.1	22
270	H2O2 decomposition mechanism and its oxidative desulfurization activity on hexagonal boron nitride monolayer: A density functional theory study. Journal of Molecular Graphics and Modelling, 2018, 84, 166-173.	1.3	22

#	Article	IF	CITATIONS
271	Amorphous Bimetallic Phosphate–Carbon Precatalyst with Deep Self-Reconstruction toward Efficient Oxygen Evolution Reaction and Zn–Air Batteries. ACS Sustainable Chemistry and Engineering, 2021, 9, 5345-5355.	3.2	22
272	Unraveling the mechanism of CO ₂ capture and separation by porous liquids. RSC Advances, 2020, 10, 42706-42717.	1.7	22
273	Oxygen vacancies mediated Bi12O17Cl2 ultrathin nanobelts: Boosting molecular oxygen activation for efficient organic pollutants degradation. Journal of Colloid and Interface Science, 2022, 609, 23-32.	5.0	22
274	Ni x Co 3―x O 4 Nanoneedle Arrays Grown on Ni Foam as an Efficient Bifunctional Electrocatalyst for Full Water Splitting. Chemistry - an Asian Journal, 2019, 14, 480-485.	1.7	21
275	The interaction nature between hollow silica-based porous ionic liquids and CO2: A DFT study. Journal of Molecular Graphics and Modelling, 2020, 100, 107694.	1.3	21
276	Porous silver microrods by plasma vulcanization activation for enhanced electrocatalytic carbon dioxide reduction. Journal of Colloid and Interface Science, 2022, 606, 793-799.	5.0	21
277	Spontaneous Dissolution of Oxometalates Boosting the Surface Reconstruction of CoMO _{<i>x</i>} (M = Mo, V) to Achieve Efficient Overall Water Splitting in Alkaline Media. Inorganic Chemistry, 2022, 61, 2619-2627.	1.9	21
278	Oxygen vacancy triggering the broad-spectrum photocatalysis of bismuth oxyhalide solid solution for ciprofloxacin removal. Journal of Colloid and Interface Science, 2022, 626, 221-230.	5.0	21
279	Ionic Liquid Assisted Solvothermal Synthesis of Cu Polyhedron-Pattern Nanostructures and Their Application as Enhanced Nanoelectrocatalysts for Glucose Detection. European Journal of Inorganic Chemistry, 2011, 2011, 1361-1365.	1.0	20
280	Plasmonicâ€enhanced visibleâ€lightâ€driven photocatalytic activity of Ag–AgBr synthesized in reactable ionic liquid. Journal of Chemical Technology and Biotechnology, 2012, 87, 1626-1633.	1.6	20
281	Preparation of 1D CuO Nanorods by Means of a Metal Ion Containing Ionic Liquid and Their Supercapacitance. European Journal of Inorganic Chemistry, 2013, 2013, 2315-2323.	1.0	20
282	Tailoring of crystalline structure of carbon nitride for superior photocatalytic hydrogen evolution. Journal of Colloid and Interface Science, 2019, 556, 324-334.	5.0	20
283	Construction of NH2-MIL-125(Ti) nanoplates modified Bi2WO6 microspheres with boosted visible-light photocatalytic activity. Research on Chemical Intermediates, 2020, 46, 3311-3326.	1.3	20
284	Minireview on the Commonly Applied Copper-Based Electrocatalysts for Electrochemical CO ₂ Reduction. Energy & Fuels, 2021, 35, 8585-8601.	2.5	20
285	Facet-dependent CdS/Bi ₄ TaO ₈ Cl Z-scheme heterojunction for enhanced photocatalytic tetracycline hydrochloride degradation and the carrier separation mechanism study <i>via</i> single-particle spectroscopy. Inorganic Chemistry Frontiers, 2022, 9, 2252-2263.	3.0	20
286	One-pot synthesis of ordered mesoporous silica encapsulated polyoxometalate-based ionic liquids induced efficient desulfurization of organosulfur in fuel. RSC Advances, 2015, 5, 76048-76056.	1.7	19
287	Designing Visibleâ€Lightâ€Driven Zâ€scheme Catalyst 2D gâ€C ₃ N ₄ /Bi ₂ MoO ₆ : Enhanced Photodegradation Activity of Organic Pollutants. Physica Status Solidi (A) Applications and Materials Science, 2018, 215, 1800520.	0.8	19
288	Highly efficient photosynthesis of H ₂ O ₂ <i>via</i> two-channel pathway photocatalytic water splitting. Inorganic Chemistry Frontiers, 2022, 9, 1701-1707.	3.0	19

#	Article	IF	CITATIONS
289	Synthesis of Multiwalled Carbon Nanotube Modified BiOCl Microspheres with Enhanced Visible‣ight Response Photoactivity. Clean - Soil, Air, Water, 2016, 44, 781-787.	0.7	18
290	Designing Zâ€scheme 2Dâ€C ₃ N ₄ /Ag ₃ VO ₄ hybrid structures for improved photocatalysis and photocatalytic mechanism insight. Physica Status Solidi (A) Applications and Materials Science, 2017, 214, 1600946.	0.8	18
291	Amorphous TiO2-supported Keggin-type ionic liquid catalyst catalytic oxidation of dibenzothiophene in diesel. Petroleum Science, 2018, 15, 870-881.	2.4	18
292	Interfacial self-assembly of monolayer Mg-doped NiO honeycomb structured thin film with enhanced performance for gas sensing. Journal of Materials Science: Materials in Electronics, 2018, 29, 11498-11508.	1.1	18
293	Ultrathin graphitic carbon nitride modified PbBiO2Cl microspheres with accelerating interfacial charge transfer for the photodegradation of organic contaminants. Colloids and Surfaces A: Physicochemical and Engineering Aspects, 2019, 582, 123804.	2.3	18
294	The construction of a Fenton system to achieve in situ H2O2 generation and decomposition for enhanced photocatalytic performance. Inorganic Chemistry Frontiers, 2019, 6, 1490-1500.	3.0	18
295	Few Layer g-C ₃ N ₄ Dispersed Quaternary Phosphonium Ionic Liquid for Highly Efficient Catalytic Oxidative Desulfurization of Fuel. Energy & Fuels, 2020, 34, 12379-12387.	2.5	18
296	Self-templated formation of (NiCo) ₉ S ₈ yolk–shelled spheres for high-performance hybrid supercapacitors. Nanoscale, 2020, 12, 23497-23505.	2.8	18
297	Mechanistic Insight into Energyâ€Transfer Dynamics and Color Tunability of Na ₄ CaSi ₃ O ₉ :Tb ³⁺ ,Eu ³⁺ for Warm White LEDs. Chemistry - A European Journal, 2020, 26, 5619-5628.	1.7	18
298	Rational Design of Caprolactam-Based Deep Eutectic Solvents for Extractive Desulfurization of Diesel Fuel and Mechanism Study. ACS Sustainable Chemistry and Engineering, 2022, 10, 4551-4560.	3.2	18
299	Synergy between plasmonic and sites on gold nanoparticle-modified bismuth-rich bismuth oxybromide nanotubes for the efficient photocatalytic C C coupling synthesis of ethane. Journal of Colloid and Interface Science, 2022, 616, 649-658.	5.0	18
300	Enhanced Oxidative Desulfurization of Dibenzothiophene by Functional Mo ontaining Mesoporous Silica. Chemical Engineering and Technology, 2015, 38, 117-124.	0.9	17
301	WO ₃ nanorod photocatalysts decorated with few-layer g-C ₃ N ₄ nanosheets: controllable synthesis and photocatalytic mechanism research. RSC Advances, 2016, 6, 80193-80200.	1.7	17
302	Investigation of Amine-Based Ternary Deep Eutectic Solvents for Efficient, Rapid, and Reversible SO ₂ Absorption. Energy & Fuels, 2021, 35, 20406-20410.	2.5	17
303	Production of 5â€Hydroxymethylfurfural from Fructose in Ionic Liquid Efficiently Catalyzed by Cr(III)â€Al ₂ O ₃ Catalyst. Chinese Journal of Chemistry, 2014, 32, 434-442.	2.6	16
304	Construction of 3D Hierarchical GO/MoS 2 /gâ€C 3 N 4 Ternary Nanocomposites with Enhanced Visibleâ€Light Photocatalytic Degradation Performance. ChemistrySelect, 2019, 4, 7123-7133.	0.7	16
305	Controllable synthesis of functionalized ordered mesoporous silica by metal-based ionic liquids, and their effective adsorption of dibenzothiophene. RSC Advances, 2014, 4, 40588-40594.	1.7	15
306	In situ growth of Ag/AgCl on the surface of CNT and the effect of CNT on the photoactivity of the composite. New Journal of Chemistry, 2015, 39, 5540-5547.	1.4	15

#	Article	IF	CITATIONS
307	Significant improvement of photocatalytic activity of porous graphitic-carbon nitride/bismuth oxybromide microspheres synthesized in an ionic liquid by microwave-assisted processing. Materials Science in Semiconductor Processing, 2015, 32, 117-124.	1.9	15
308	Hexacyanoferrateâ€based ionic liquids as Fentonâ€like catalysts for deep oxidative desulfurization of fuels. Applied Organometallic Chemistry, 2016, 30, 753-758.	1.7	15
309	Single layer twoâ€dimensional Oâ€gâ€C ₃ N ₄ : An efficient photocatalyst for improved molecular oxygen activation ability. Physica Status Solidi (A) Applications and Materials Science, 2017, 214, 1600704.	0.8	15
310	Electronic state tuning over Mo-doped W18O49 ultrathin nanowires with enhanced molecular oxygen activation for desulfurization. Separation and Purification Technology, 2022, 294, 121167.	3.9	15
311	Efficient degradation of methylene blue dye by catalytic oxidation using the Na8Nb6O19·13H2O/H2O2 system. Korean Journal of Chemical Engineering, 2011, 28, 1126-1132.	1.2	14
312	Preparation of metal ions impregnated polystyrene resins for adsorption of antibiotics contaminants in aquatic environment. Journal of Applied Polymer Science, 2015, 132, .	1.3	14
313	Metalâ€based ionic liquid assisted synthesis of highly dispersed mesoporous Fe(III)/SiO ₂ for enhanced adsorption of antibiotics. Journal of Chemical Technology and Biotechnology, 2019, 94, 3815-3824.	1.6	14
314	Highly Efficient Adsorption of Oils and Pollutants by Porous Ultrathin Oxygen-Modified BCN Nanosheets. ACS Sustainable Chemistry and Engineering, 2019, 7, 3234-3242.	3.2	14
315	Metal Nanoparticles Confined within an Inorganic–Organic Framework Enable Superior Substrate-Selective Catalysis. ACS Applied Materials & Interfaces, 2020, 12, 42739-42748.	4.0	14
316	Reactable ionic liquidâ€assisted solvothermal synthesis of flowerâ€like bismuth oxybromide microspheres with highly visibleâ€light photocatalytic performances. Micro and Nano Letters, 2013, 8, 450-454.	0.6	13
317	Controllable Synthesis of Ultrathin NiCo ₂ O ₄ Nanosheets Incorporated onto Composite Nanotubes for Efficient Oxygen Reduction. Chemistry - an Asian Journal, 2017, 12, 2426-2433.	1.7	13
318	Promoting Pt catalysis for CO oxidation <i>via</i> the Mott–Schottky effect. Nanoscale, 2019, 11, 18568-18574.	2.8	13
319	Partial Oxidation of Sn2+ Induced Oxygen Vacancy Overspread on the Surface of SnO2â^'x/g-C3N4 Composites for Enhanced LED-Light-Driven Photoactivity. Journal of Inorganic and Organometallic Polymers and Materials, 2019, 29, 765-775.	1.9	13
320	Engineering Highly Dispersed Pt Species by Defects for Boosting the Reactive Desulfurization Performance. Industrial & amp; Engineering Chemistry Research, 2021, 60, 2828-2837.	1.8	13
321	Nanostructure and functional group engineering of black phosphorus via plasma treatment for CO2 photoreduction. Journal of CO2 Utilization, 2021, 54, 101745.	3.3	13
322	Fabrication and characterization of visible-light-induced photocatalyst Gd2O3/Ag3VO4. Reaction Kinetics, Mechanisms and Catalysis, 2010, 99, 471.	0.8	12
323	Cerium Oxysulfide with O–Ce–S Bindings for Efficient Adsorption and Conversion of Lithium Polysulfide in Li–S Batteries. Inorganic Chemistry, 2021, 60, 12847-12854.	1.9	12
324	Supported phosphotungstic-based ionic liquid as an heterogeneous catalyst used in the extractive coupled catalytic oxidative desulfurization in diesel. Research on Chemical Intermediates, 2019, 45, 4315-4334.	1.3	11

#	Article	IF	CITATIONS
325	Theoretical prediction of F-doped hexagonal boron nitride: A promising strategy to enhance the capacity of adsorptive desulfurization. Journal of Molecular Graphics and Modelling, 2020, 101, 107715.	1.3	11
326	Plasma-induced black bismuth tungstate as a photon harvester for photocatalytic carbon dioxide conversion. New Journal of Chemistry, 2021, 45, 1993-2000.	1.4	11
327	Orientated dominating charge separation via crystal facet homojunction inserted into BiOBr for solar-driven CO2 conversion. Journal of CO2 Utilization, 2022, 59, 101957.	3.3	11
328	Electrochemical and Transport Characteristics of V(II)/V(III) Redox Couple in a Nonaqueous Deep Eutectic Solvent: Temperature Effect. Journal of Energy Engineering - ASCE, 2017, 143, .	1.0	10
329	Polyoxometalate-based silica-supported ionic liquids for heterogeneous oxidative desulfurization in fuels. Petroleum Science, 2018, 15, 882-889.	2.4	10
330	Synthesis of amphiphilic peroxophosphomolybdates for oxidative desulfurization of fuels in ionic liquids. Petroleum Science, 2018, 15, 890-897.	2.4	10
331	Ionic liquid-induced preparation of novel CNTs/PbBiO2Cl nanosheet photocatalyst with boosted photocatalytic activity for the removal of organic contaminants. Colloids and Surfaces A: Physicochemical and Engineering Aspects, 2022, 634, 127894.	2.3	10
332	Ultrathin structure of oxygen doped carbon nitride for efficient CO ₂ photocatalytic reduction. Nanotechnology, 2022, 33, 115404.	1.3	10
333	Branch-Regulated Palladium–Antimony Nanoparticles Boost Ethanol Electro-oxidation to Acetate. Inorganic Chemistry, 2022, 61, 6337-6346.	1.9	10
334	Light irradiation induced aerobic oxidative deep-desulfurization of fuel in ionic liquid. RSC Advances, 2015, 5, 99927-99934.	1.7	9
335	Homogeneous synthesis of linoleic acidâ€grafted chitosan oligosaccharide in ionic liquid and its selfâ€assembly performance in aqueous solution. Journal of Applied Polymer Science, 2015, 132, .	1.3	9
336	Fe ₂ O ₃ Nanoparticles Modified 2D Nâ€Doped Porous Grapheneâ€like Carbon as an Efficient and Robust Electrocatalyst for Oxygen Reduction Reaction. ChemistrySelect, 2019, 4, 4131-4139.	0.7	9
337	Oneâ€step Mechanical Synthesis of Oxygenâ€defect Modified Ultrathin Bi ₁₂ O ₁₇ Br ₂ Nanosheets for Boosting Photocatalytic Activity. ChemistrySelect, 2020, 5, 11177-11184.	0.7	9
338	Self-assembly and boosted photodegradation properties of perylene diimide <i>via</i> different solvents. New Journal of Chemistry, 2021, 45, 21701-21707.	1.4	9
339	Peroxo-tungsten complex catalysed synthesis of adipic acid and benzoic acid with hydrogen peroxide. Journal of Chemical Research, 2006, 2006, 774-775.	0.6	8
340	Graphene quantum dots modified Ag ₃ PO ₄ for facile synthesis and the enhanced photocatalytic performance. Journal of the Chinese Advanced Materials Society, 2018, 6, 255-269.	0.7	8
341	The synthesis of Fe-containing ionic liquid and its catalytic performance for the dehydration of fructose. Chemical Papers, 2017, 71, 1541-1549.	1.0	7
342	Porous-C3N4 with High Ability for Selective Adsorption and Photodegradation of Dyes Under Visible-Light. Journal of Inorganic and Organometallic Polymers and Materials, 2017, 27, 1674-1682.	1.9	7

#	Article	IF	CITATIONS
343	Metal ion-containing ionic liquid assisted synthesis and enhanced photoelectrochemical performance of g-C ₃ N ₄ /ZnO composites. Materials Technology, 2018, 33, 185-192.	1.5	7
344	Construction of cobaltous oxide/nickel–iron oxide electrodes with great cycle stability and high energy density for advanced asymmetry supercapacitor. Journal of Materials Science: Materials in Electronics, 2019, 30, 21219-21228.	1.1	7
345	Rational Design of Porous TiO ₂ @Nâ€Doped Carbon for High Rate Lithiumâ€ion Batteries. Energy Technology, 2019, 7, 1800911.	1.8	7
346	Shortâ€ŧime Thermal Oxidation of Ultrathin and Broadband Carbon Nitride for Efficient Photocatalytic H ₂ Generation. ChemCatChem, 2020, 12, 1169-1176.	1.8	7
347	Assessing the Maximum Power and Consistency of Carbon Supercapacitors Through a Facile Practical Strategy. ACS Sustainable Chemistry and Engineering, 2020, 8, 12430-12436.	3.2	7
348	In situ preparation of Bi2O3/(BiO)2CO3 composite photocatalyst with enhanced visible-light photocatalytic activity. Research on Chemical Intermediates, 2021, 47, 1601-1613.	1.3	7
349	One-pot synthesis and characterization of tungsten-containing meso-ceria with enhanced heterogenous oxidative desulfurization in fuels. RSC Advances, 2016, 6, 68922-68928.	1.7	6
350	One-pot ionic liquid-assisted strategy for GO/BiOI hybrids with superior visible-driven photocatalysis and mechanism research. Materials Technology, 2017, 32, 131-139.	1.5	6
351	Double regulation of bismuth and halogen source for the preparation of bismuth oxybromide nanosquares with enhanced photocatalytic activity. Journal of Colloid and Interface Science, 2017, 492, 25-32.	5.0	6
352	A novel carbon quantum dots (CQDs) modified Cs4PW11O39Fe(III)(H2O) material to achieve high photocatalytic property. Functional Materials Letters, 2020, 13, 2051022.	0.7	6
353	Surface Engineering of 2D Carbon Nitride with Cobalt Sulfide Cocatalyst for Enhanced Photocatalytic Hydrogen Evolution. Physica Status Solidi (A) Applications and Materials Science, 2021, 218, 2100012.	0.8	6
354	Positively charged silver improve carbon dioxide electroreduction reaction performance by introducing phosphate. Journal of Colloid and Interface Science, 2022, 609, 65-74.	5.0	6
355	Metastable Antimonyâ€Doped SnO ₂ Quantum Wires for Ultrasensitive Gas Sensors. Advanced Electronic Materials, 2022, 8, .	2.6	6
356	Fabrication of dual-mesoporous silica by triblock copolymers and metal-based ionic liquid: efficient and durable catalyst for oxidative desulfurization in fuel. RSC Advances, 2015, 5, 104322-104329.	1.7	5
357	Fabrication of functional dual-mesoporous silicas by using peroxo-tungstate ionic liquid and their applications in oxidative desulfurization. Journal of Porous Materials, 2015, 22, 1227-1233.	1.3	5
358	Controllable preparation of highly dispersed TiO ₂ nanoparticles for enhanced catalytic oxidation of dibenzothiophene in fuels. Applied Organometallic Chemistry, 2018, 32, e4351.	1.7	5
359	SBA-15 supported molybdenum oxide towards efficient catalytic oxidative desulfurization: effect of calcination temperature of catalysts. Journal of the Chinese Advanced Materials Society, 2018, 6, 44-54.	0.7	5
360	Controlled synthesis of novel PbBiO2I microsphere structure towards photocatalytic degradation of bisphenol A. Research on Chemical Intermediates, 2018, 44, 5879-5891.	1.3	5

#	Article	IF	CITATIONS
361	Sizeâ€Dependent Activity of Ironâ€Nickel Oxynitride towards Electrocatalytic Oxygen Evolution. ChemNanoMat, 2019, 5, 883-887.	1.5	5
362	Rambutanâ€Inspired Yolkâ€Shell Silica@Carbon Frameworks from Biomass for Longâ€Life Anode Materials. ChemistrySelect, 2019, 4, 14075-14081.	0.7	5
363	Controllable synthesis of FeWO4/BiOBr in reactive ionic liquid with effective charge separation towards photocatalytic pollutant removal. Research on Chemical Intermediates, 2019, 45, 437-451.	1.3	5
364	Bipolar Organic Material Assisted Surface and Boundary Defects Passivation for Highly Efficient MAPbI 3 â€Based Inverted Perovskite Solar Cells. Solar Rrl, 2020, 4, 2000369.	3.1	5
365	Strong electronic coupled FeNi ₃ /Fe ₂ (MoO ₄) ₃ nanohybrids for enhancing the electrocatalytic activity for the oxygen evolution reaction. Inorganic Chemistry Frontiers, 2020, 7, 2791-2798.	3.0	5
366	Novel ionic liquid modified carbon nitride fabricated by in situ pyrolysis of 1-butyl-3-methylimidazolium cyanamide to improve electronic structure for efficiently degradation of bisphenol A. Colloids and Surfaces A: Physicochemical and Engineering Aspects, 2021, 610, 125648.	2.3	5
367	Ionic Liquid-Assisted Synthesis of Ag3PO4 Spheres for Boosting Photodegradation Activity under Visible Light. Catalysts, 2021, 11, 788.	1.6	5
368	Dual modulation steering electron reducibility and transfer of bismuth molybdate nanoparticle to boost carbon dioxide photoreduction to carbon monoxide. Journal of Colloid and Interface Science, 2022, 610, 518-526.	5.0	5
369	Graphene-like BN/BiOBr composite: synthesis via a reactable ionic liquid and enhanced visible light photocatalytic performance. Materials Technology, 2016, 31, 463-470.	1.5	4
370	Steering Hole Transfer from the Light Absorber to Oxygen Evolution Sites for Photocatalytic Overall Water Splitting. Advanced Materials Interfaces, 0, , 2101158.	1.9	4
371	Partitioning behavior of tetracycline in hydrophobic ionic liquids two-phase systems. Separation Science and Technology, 2015, , 150527095459001.	1.3	3
372	Construction of a 2D Graphene-Like MoS2 /C3 N4 Heterojunction with Enhanced Visible-Light Photocatalytic Activity and Photoelectrochemical Activity. Chemistry - A European Journal, 2016, 22, 4645-4645.	1.7	3
373	Solar driven high efficiency hydrogen evolution catalyzed by surface engineered ultrathin carbon nitride. New Journal of Chemistry, 2020, 44, 19314-19322.	1.4	3
374	High-performance mesoporous γ-Fe2O3 sphere/graphene aerogel composites towards enhanced lithium storage. Nanotechnology, 2020, 31, 265405.	1.3	3
375	Activation of Fe species on graphitic carbon nitride nanotubes for efficient photocatalytic ammonia synthesis. International Journal of Energy Research, 2022, 46, 13453-13462.	2.2	3
376	Controlled growth of BaMoO4 hierarchical superstructures in functionalized ionic liquids. Pure and Applied Chemistry, 2009, 81, 2355-2367.	0.9	2
377	Graphene-Analogue Boron Nitride Modified Bismuth Oxyiodide with Increased Visible-Light Photocatalytic Performance. Physica Status Solidi (A) Applications and Materials Science, 2018, 215, 1800146.	0.8	2
378	The electronic structure and physicochemical property of boron nitridene. Journal of Molecular Graphics and Modelling, 2020, 94, 107475.	1.3	2

#	Article	IF	CITATIONS
379	Highly dispersed tungsten-based quantum dots confined in porous channel induced by ionic liquid with remarkable desulfurization behavior. Separation and Purification Technology, 2021, , 119676.	3.9	2

Hydrogels: Reversible Formation of gâ€C₃N₄ 3D Hydrogels through Ionic Liquid Activation: Gelation Behavior and Roomâ€Temperature Gasâ€Sensing Properties (Adv. Funct. Mater.) Tj ETQq0 0 0**7g**BT /Overlock 10 Tf

381	Facile preparation of monolayer NiO thin film for high performance THF sensor. Journal of the Chinese Advanced Materials Society, 2018, 6, 1-7.	0.7	1
382	Integration of metallic TaS ₂ Coâ€catalyst on carbon nitride photoharvester for enhanced photocatalytic performance. Canadian Journal of Chemical Engineering, 2019, 97, 1821-1827.	0.9	1
383	Preparation and photocatalytic performance of metallic Nb0.9Ta0.1S2/2D-C3N4 composite. Oxford Open Materials Science, 2020, 1, .	0.5	1
384	Frontispiece: Mechanistic Insight into Energyâ€Transfer Dynamics and Color Tunability of Na ₄ CaSi ₃ O ₉ :Tb ³⁺ ,Eu ³⁺ for Warm White LEDs. Chemistry - A European Journal, 2020, 26, .	1.7	0
385	Constructing Ni 3 C/2D g 3 N 4 Photocatalyst and the Internal Catalytic Mechanism Study. Physica Status Solidi (A) Applications and Materials Science, 2021, 218, 2100171.	0.8	0
386	Facile Construction of Magnetic Ionic Liquid Supported Silica for Aerobic Oxidative Desulfurization in Fuel. Catalysts, 2021, 11, 1496.	1.6	0
387	Interface engineering of quaternary ammonium phosphotungstate for efficient oxidative desulfurization of high-sulfur petroleum coke. Petroleum Science and Technology, 2023, 41, 86-103.	0.7	0
388	A novel Sillén-structured Bi-based oxybromide: CdBiO ₂ Br ultrathin nanosheets for enhanced photocatalytic activity. Environmental Technology (United Kingdom), 0, , 1-15.	1.2	0